Drivers of erosion and suspended sediment transport in three headwater catchments of the Mexican Central Highlands

Clément Duvert, Nicolas Gratiot, O. Evrard, Oldrich Navratil, Julien Némery, Christian Prat, Michel Esteves

Drivers of erosion and suspended sediment transport in three headwater catchments of the Mexican Central Highlands

Clément Duvert [a, b, *], Nicolas Gratiot [a], Olivier Evrard [c], Oldrich Navratil [a], Julien Némery [a], Christian Prat [a], Michel Esteves [a]

[a] Laboratoire d'étude des Transferts en Hydrologie et Environnement (LTHE) – IRD, G-INP, Université de Grenoble 1, CNRS, Grenoble, France

[b] Centro de Investigaciones en Geografía Ambiental, Universidad Nacional Autónoma de México, Morelia, Mexico

[c] Laboratoire des Sciences du Climat et de l'Environnement (LSCE/IPSL) – Unité Mixte de Recherche 8212 – CEA, CNRS, UVSQ, Gif-sur-Yvette, France

* Corresponding author. Tel.: +334 76 63 55 39; Fax: +334 76 82 50 14; E-mail: clement.duvert@gmail.com

Abstract

Quantifying suspended sediment exports from catchments and understanding suspended sediment dynamics within river networks is important in areas draining erodible material that contributes to the siltation of downstream reservoirs and to the degradation of water quality. A one-year continuous monitoring study of water and sediment fluxes was conducted in three upland subcatchments (3.0, 9.3, and 12.0 km^2) located within the Cointzio basin, in the central volcanic highlands of Mexico (Michoacán state). Two subcatchments generated high sediment exports (i.e., Huertitas, 900-1500 t.km^{-2}.y^{-1} and Potrerillos, 600-800 t.km^{-2}.y^{-1}), whereas the third subcatchment was characterized by a much lower sediment yield (i.e., La Cortina, 30 t.km^{-2}.y^{-1}). Such disparities in subcatchment behaviours were associated with the presence of severely gullied areas in Huertitas and Potrerillos rather than with rainfall erosivity indices. An adapted classification of hysteretic patterns between suspended sediment concentration (SSC) and discharge was proposed because 42% of flood events contributing to 70% of sediment export were not discriminated by the classical clockwise/anticlockwise typology. This new classification allowed identification of relationships in the hydrosedimentary responses of successive floods. A stream transport capacity limit was also detected during hydrograph recession phases. Overall, hydrosedimentary processes proved to be seasonally dependent: sediment export was repeatedly limited by the stream transport capacity during the first part of the rainy season, whereas a channel minimum erosivity threshold was frequently reached at the end of the season.

Keywords: sediment yield; rainy season; sediment-discharge hysteresis; mountainous catchments; volcanic soils.

1. Introduction

Accelerated soil erosion and subsequent fine sediment delivery to rivers are two major environmental issues that increasingly concern land and water management authorities throughout the world (Ongley, 1996). Soil loss is commonly associated with arable land depletion and thus with a reduction in crop yields (Pimentel et al., 1995). In addition to on-site effects, fine sediment supply leads to severe off-site impacts: Sediment can accumulate on the riverbed and increase flooding potential, decrease reservoir storage capacity, and degrade aquatic ecosystems by increasing water turbidity and by mobilizing associated contaminants (Newcombe and McDonald, 1991; Owens et al., 2005).

Upland areas are known to be important contributors to fine sediment production and delivery to downstream reaches. Indeed, they often act as sediment source areas because of their steep and deeply incised morphology (Dietrich and Dunne, 1978; Walling and Webb, 1996; Sidle et al., 2000). Therefore, understanding the processes governing the release of fine sediment from headwater catchments to lowland water bodies is essential. The analysis also requires appreciation of the temporal and spatial variations in upland-lowland linkages, as determined by (i) historic land use changes that often continue to influence contemporary sediment dynamics (e.g., Wasson et al., 1998; Kasai et al., 2005), and (ii) by the extent of connectivity between hillslopes and downstream reaches, i.e., significance of sediment storage within channels, floodplains and reservoirs (e.g., Fryirs and Brierley, 1999; Lang et al., 2003).

Various methods have been proposed in recent decades that investigate fine sediment transport. Benefiting from the development of automated monitoring stations, numerous studies have described the pattern of suspended sediment concentration during single hydrologic events (e.g., Webb and Walling, 1982; Walling and Webb, 1983; Klein, 1984; Jeje et al., 1991; Mano et al., 2009). These works showed that, in most streams, the bulk of sediment is transported during single floods and that the relationship between suspended sediment concentration (SSC) and water discharge (*Q*) during a storm is highly variable. Resulting SSC-*Q* hysteresis patterns have been widely examined at the event scale in order to interprete geomorphic processes occurring within catchments and to outline the spatial distribution of sediment sources (e.g., Klein, 1984; Williams, 1989; Lenzi and Marchi, 2000; Jansson, 2002). This integrative tool is still frequently used in recent literature (e.g., Lefrançois et al., 2007; Sadeghi et al., 2008; López-Tarazón et al., 2009; Smith and Dragovich, 2009). Another increasingly used approach for the understanding of mechanisms controlling sediment delivery consists in establishing statistical correlations between SSC and a set of parameters such as, for instance, rainfall intensity, moisture initial conditions, sediment load, and peak discharge (Seeger et al., 2004; Zabaleta et al., 2007; Nadal-Romero et al., 2008; Oeurng et al., 2010). Still, such statistical methods may be usefully employed together with physically based approaches to improve the understanding of sediment dynamics in headwater catchments.

A large part of the global problems and the unresolved issues mentioned above are experienced in the Mexican Central Plateau, which concentrates the majority of the country's population (INEGI, 2006). This area underwent significant land use changes during the last decades that induced an intensification of soil erosion (SEMARNAT-CP, 2003). This leads in turn to the degradation of surface water bodies and consequently to enhanced water treatment costs (Vidal et al., 1985; Alcocer and Escobar, 1993). This situation is particularly acute in the volcanic region located around Morelia (capital of Michoacán state, ca. 1 million inhabitants).

Recent studies conducted in central Mexico provided significant insights about erosion processes and soil loss at plot, hillslope, or subcatchment scales (e.g., Servenay and Prat, 2003; Descroix et al., 2008; Viramontes et al., 2008; Bravo-Espinosa et al., 2009; Vásquez-Méndez et al., 2010). However, so far, very few studies have addressed the question of sediment delivery to rivers and sediment yields in Mexican basins (Ramírez-León and Aparicio, 2009). This paper reports the results of high frequency monitoring of discharge and suspended sediment carried out in the Cointzio basin, close to the city of Morelia. Three headwater subcatchments of the basin (i.e., La Cortina, Huertitas, and Potrerillos) with distinct characteristics (soil type, slope gradient, land use) were equipped and surveyed all throughout 2009 to provide the first assessment of the suspended sediment dynamics in volcanic mountainous headwaters of the Mexican plateau.

The objectives of our work were (i) to quantify the fine sediment loss at the subcatchment scale and compare the sensitivity to erosion of the three study sites, (ii) to point out advantages and disadvantages of our high frequency monitoring for potential applications in other similar conditions, and (iii) to enlarge the scope of our findings by identifying the dominant processes driving suspended sediment transport in 1-10 km^2 scale mountainous subcatchments under subhumid conditions.

2. Material and methods

2.1. Study area

The Cointzio River basin is located in the southern part of the Mexican Central Plateau, where it meets the Trans-Mexican Volcanic Belt (Fig. 1). The region has a temperate subhumid climate characterized by two contrasting seasons: the dry season lasting from November to May and the wet season between June and October. Mean annual rainfall reaches 770 mm in Morelia (period 1975-2005). Nearly 80% of the precipitation occurs during the five months of the rainy season (Carlón-Allende et al., 2009). Rainfall is generally dominated by high intensity localized storms, although less intense and more widespread events also repeatedly occur.

The Cointzio River basin drains an area of 630 km^2 with altitudes ranging from 3 440 m at the summit to 1 990 m at the outlet. The main watercourse is the *Rio Grande de Morelia* river, which originates from moderate hillslopes in the eastern part of the basin and flows across it until reaching the man-made reservoir of Cointzio (4 km^2, 65 Mm^3) located at the outlet. The reservoir was built in 1940 to provide water for domestic consumption and agricultural needs. Given that it currently supplies 25% of the water distributed in Morelia, its increasing siltation is a major concern for the region (Susperregui et al., 2009).

Geology of the upper basin mainly consists of basalt and andesitic rocks produced by Quaternary volcanic activity. The lower part of the area is underlain by alluvium and lacustrine deposits. The presence of igneous material led to the formation of fine-textured soils. Schematically, Andisols (i.e., black fertile soils formed in volcanic silicate-rich ash) are prominent in upland parts of the basin, Acrisols (i.e., red acid soils with high clay content) on the hillslopes and Luvisols (i.e., weathered soils with accumulation of clay in a subsurface horizon) in the lowlands (FAO, 2006). Both

Andisols and Acrisols are known to be poorly resistant to water erosion when they undergo land use changes (Poulenard et al., 2001; Bravo-Espinosa et al., 2009).

Hydrosedimentary fluxes were measured throughout 2009 with a high frequency (i.e., 5-min) at the outlet of the three headwater catchments of the Cointzio basin; i.e., Huertitas (3.0 km^2), La Cortina (9.3 km^2), and Potrerillos (12.0 km^2) (Fig. 1). These three sites are characterized by contrasted landforms, morphologies, and soil types, as detailed hereafter:

Huertitas and La Cortina are located in the eastern mountains of the basin. La Cortina is underlain by Andisols, rich in organic matter and characterized by an excellent microstructure under wet conditions. It constitutes a local reference in terms of good ecological status. Its undulating landscape (mean slope 12%) is mainly covered by forests (52%) and maize/avocado fields (46%; Table 1).

The Huertitas subcatchment (mean slope 18%) covers a lower range of altitudes and relies exclusively on Acrisols. The catchment displays a severely gullied landscape on 6% of its area, with sparse vegetation and soils highly sensitive to water erosion (Fig. 2; Table 1). Land use mainly consists of rangeland (65%) and cropland (28%).

Potrerillos is located in the southern part of the Cointzio basin, at the piedmont of a volcanic formation (mean slope 15%), and soils are mainly Acrisols (60%) and Andisols (40%). Channel incision and gullies are connected throughout the subcatchment as in Huertitas. These degraded areas affect 1% of the subcatchment. Land use in Potrerillos consists of a combination of cropland (40%), forests (37%) and grassland (23%; Table 1). The three study sites are therefore representative of the variety of environments found in upstream areas of Cointzio.

The river draining La Cortina is permanent with a substantial flow that is even observed during the dry winter months. In Huertitas, waterflow is also perennial but the baseflow contribution is very low in winter. In Potrerillos, the river is ephemeral and only active during the five months of the rainy season.

Grain size of the suspended sediment transported in the subcatchments varies according to the location and to the type of flood, but it is predominantly clay- and silt-sized.

2.2. Field monitoring

2.2.1. Water discharge and suspended sediment measurements

Two of the three monitoring sites (i.e., Huertitas and La Cortina) consist of a stable channel section built of concrete and installed for this study. The third monitored site (i.e., Potrerillos) was installed under a bridge. It is made up of a rectangular section underlain by bedrock outcrops, and the local topography leads to phases of sediment deposition and resuspension. This required careful data processing.

Water level was measured at a 5-min time step with Thalimede® OTT water level gauges. At each station, between 10 and 15 discharge measurements were carried out using the tracer dilution gauging method. Water discharge time series were determined using continuous water level records and rating curves obtained by the dilution method (see the technical note of Duvert, 2009, for details about the methodology used and its associated uncertainties).

Time series of SSC were calculated using stage-triggered Teledyne ISCO® 3700 automatic water samplers containing 24 bottles of 1 liter each. At all sites, suspended sediment sampling was performed at a depth of about 10 cm from the streambed and it did not vary with stage. Suspended sediment concentrations under baseflow conditions were also surveyed by means of manual samples collected daily around 6 p.m. by local staff. The use of automatic turbidity sensors would have been preferable in the three upland subcatchments. However, during the equipment installation phase in 2008, it became apparent that this option was not feasible because of numerous field constraints. Indeed, sedimentation frequently occurred in river sections at the outlet, and the water depth in the channel was not sufficient during baseflow.

A Campbell CR800® datalogger was programmed to trigger sampling based on a stage-variation threshold and using the following strategy: stations were visited every week for collecting samples and replacing bottles when necessary; given this operational constraint, we followed a trial-and-error process described by Gao (2008). Water level monitoring had also been conducted throughout 2008 at the three stations (data not reported in this paper); we used these time series to simulate an optimized sampling frequency. The aim was to obtain reliable load estimates during small events without oversampling large events in order to avoid exhausting the samplers' available bottles. At all sites, the most appropriate water depth threshold appeared to be 5 cm for 5-min time step requests. The algorithm checked whether water depth variation (either positive or negative) exceeded 5 cm for each time step. When this condition was fulfilled, sampling was initiated. The water depth value was then stored until again reaching variations of ± 5 cm in the following time steps. The sampling conducted in 2009 confirmed the relevance of this setting: on average, 10 to 15 samples were collected weekly in each station, and we were only confronted with an exhaustion of the 24 bottles on two occasions.

Collected samples were filtered in the laboratory of CIGA-UNAM in Morelia using preweighed Standard Durieux® 0.7-µm-diameter glass microfiber filter papers. The filters were then dried for 2 h at 105°C and weighed with a high precision balance (uncertainty ± 0.1 mg). In case of very high SSC, a known volume of sample was dried during 24 h at 60°C and the residue was weighed. In this paper, all SSC measurements refer to total suspended sediment (i.e., comprising mineral and organic fractions).

Annual suspended sediment yield (SSY, in tons) measured in 2009 was calculated using Eq. (1):

$$SSY = 0.3 \cdot \sum_{i=1}^{n} (Q \cdot SSC) \qquad (1)$$

where SSC is the suspended sediment concentration (g.L^{-1}) (corresponding to a 5-min frequency linear interpolation of data from automatic sampler and from manual sampling), Q is the instantaneous discharge (m^3.s^{-1}) (5-min frequency), and n corresponds to the number of 5-min intervals within a year.

Suspended sediment loads (SS loads) exported during single events were also estimated using Eq. 1 with n corresponding to the number of 5-min intervals during the event of interest. Finally, by calculating the ratio between the SS load and the stormflow runoff volume for each event of the rainy season, an integrative SSC was obtained per event.

In terms of monitoring efficiency, 20 out of the 23 events recorded in 2009 were fully sampled in La Cortina (i.e., 87%), 23 of 30 in Huertitas (i.e., 77%), and 33 of 41 in Potrerillos (i.e., 80%). The 30 May 2009 event that occurred in Huertitas, and that resulted in being the most intense of the season, could not be sampled because the water level floating gauge remained trapped during the rising phase (peak flow could nevertheless be documented by means of visual observation). Similarly, in Potrerillos, the highest storm event that occurred on 21 July 2009 was not sampled because of an early exhaustion of bottles. Uncertainties associated with these missing values are discussed later (section 4.1).

Grain size distribution was also determined for four storm events composite samples as an exploratory approach to link sediment yield to physical process settings. Samples were analyzed with a Malvern® particle size analyzer after being submitted to a 2-min ultrasonic agitation.

2.2.2. Uncertainties associated with suspended sediment measurements

As mentioned by Gao (2008), SSY estimates must be interpreted with care. Such calculations involve several sources of errors:

First, SSY estimates require continuous discharge data, which implies uncertainties related to (i) water depth measurements by automatic gauges, (ii) discharge measurements for the rating curve construction, and (iii) calculation of discharges from water level data through the rating curve. The sum of these uncertainties is usually considered to reach 10-20% (European ISO EN Rule 748, 1997; Navratil et al., 2009).

Second, the use of an automatic sampler and thus of a single sampling point is questionable: we assumed that, owing to the fine-grained size of sediment and to the turbulent conditions prevailing in the monitoring sites, the particles would be well mixed throughout the water column. An experimental investigation conducted by Navratil et al. (2009) reported that the use of automatic sampling combined with laboratory manipulations can lead to a ca. 20% underestimation of SSC values with an additional centered error of 10-20%.

Third, the algorithm selected for the triggering of automatic samplers introduces another bias: the representativeness of fine sediment sampling during a storm is indeed directly dependent on the algorithm capacity to adequately cover the event (i.e., did the program allow sampling during SSC peak?). Suspended sediment yield estimates depend thus on the algorithm efficiency. Furthermore, the type of interpolation used to join all SSC discrete values can be a source of additional errors.

2.2.3. Rainfall measurement

Each subcatchment was equipped with a HOBO® H07 tipping-bucket automatic rain gauge (0.2 mm/pulse). The equipment provided complete and continuous rainfall monitoring. In La Cortina and Potrerillos, 100% of the wet season was covered by rainfall data. However, in Huertitas, records were only obtained during 95% of the year because of several technical problems.

2.3. Data analysis

2.3.1. Sediment detachment

Several approaches were used to derive information on sediment dynamics from the high frequency data sets. Based on the soil detachment theory (Quansah, 1981), a first step of our analysis aimed at studying the relationship between rainfall intensity and SS load at the event scale. Various authors (e.g., Poesen, 1985) reported that rainfall kinetic energy (*KE*) can be used as an indicator of the potential ability of rain drops to detach soil. Rainfall kinetic energy was then calculated for each event as a proxy of rainfall erosivity (Salles et al., 2002), following the relation described by Brandt (1990):

$$KE_{mm} = \sum_{i} 8.95 + 8.44 \cdot \log_{10} I_i \qquad (2)$$

where KE_{mm} is the volume-specific kinetic energy ($J.m^{-2}.mm^{-1}$), and I is the rainfall intensity at the 5-min time step ($mm.h^{-1}$).

To allow detection of correlations between the set of parameters, nine quantitative variables were then derived for each rainfall–runoff event: (i) cumulative precipitation depth during the event, (ii) maximum rainfall intensity in 5 min, (iii) kinetic energy released by the rainfall, (iv) discharged volume during the stormflow event, (v) runoff coefficient, (vi) maximum instantaneous discharge, (vii) maximum SSC, (viii) mean SSC during the event, and (ix) SS load exported. Each event was also characterized by two semiquantitative parameters: (x) the slope of hydrograph rising limb and (xi) moisture/flood initial conditions (Table 2). Hydrographs were classified visually according to the velocity of their rising phase (slow/fast). Initial moisture conditions were classified using both precipitation and discharge data: a class was assigned to each event, ranging from 0 (dry) to 3 (wet+++), depending on the initial moisture conditions and on the extent of flood generation during the previous 24 h (Table 2). Finally, the type of SSC-Q hysteretic pattern was considered (xii).

When testing relationships between parameters, data scattering rapidly appeared to strongly affect the graphical analysis. Parameters were therefore plotted using bilogarithmic axes.

2.3.2. Sediment transport

Individual flood events were analyzed in terms of SSC-discharge hysteretic patterns. Processes contributing to the SS dynamics, i.e., sediment supply and remobilization of deposited sediment, occur at very short timescales (Asselman, 1999; Gomi et al., 2005). The hysteresis between SSC and discharge has been widely reported to be a useful tool providing information on sediment sources and the mechanics of sediment delivery (e.g., Jansson, 2002). In small basins, SSC usually presents a higher sensitivity to local sources such as bank collapse, concentrated sediment inputs from gullies, etc., which may complicate interpretations (Chappell et al., 1999; Lefrançois et al., 2007). On the other hand, the more homogeneous precipitation that usually characterizes small drainage areas could allow a less complex interpretation of rainfall data and, in turn, of runoff and erosion dynamics.

Floods were classified according to their hysteretic pattern. The SSC-Q diagrams were drawn with linear axes for both variables. We used an adapted version of the methodology commonly described and based on the typology of Williams (1989), which discriminates events into clockwise, counterclockwise, simultaneous and figure eight shaped hysteretic loops. This adapted classification is presented in section 3.2.2.

2.3.3. Factorial analysis

Statistical tools offer an alternative and complementary approach to assess the relationship between driving parameters and their consequences on sediment dynamics. They define objectively the degree of correlation between variables through a correlation matrix. A factorial analysis was therefore conducted on the sets of variables compiled in the three subcatchments for each flood event. Our aim was to apply a technique allowing the comparison of both quantitative and discrete parameters. The factorial analysis for mixed data (FAMD) (Escoufier, 1979; Pagès, 2004), developed in the *R* environment by Lê et al. (2008) through the FactomineR package, was selected. This type of analysis allows the extension of a multiple factor analysis to mixed sets of variables (Pagès, 2004). The RV coefficient, i.e., a multivariate generalization of the Pearson coefficient (Robert and Escoufier, 1976), was chosen to estimate correlations between variables. When variables were dependent (e.g., discharge peak and discharged volume during a flood event), only one variable was analyzed.

3. Results

3.1. Precipitation, runoff and sediment transport

3.1.1. Precipitation

At the basin scale, precipitations occurred from mid-May 2009 until late October 2009. The months of July and August were unusually dry, and the end of the rainy season (i.e., September and October) provided higher rainfall than usual. Total rainfall depth measured in the basin during 2009 reached 805 mm according to the Thiessen method and using data from nine gauges available across the Cointzio basin (Anguiano-Valencia, 2010). This value can be considered as a mean value compared to the long-term rainfall database (400-1100 $mm.y^{-1}$) available at Santiago Undameo (1954-2004), which is a station located just upstream from the Cointzio reservoir (Gratiot et al., 2010).

Significant disparities were observed among the three subcatchments: in La Cortina, annual precipitation reached 1230 mm, whereas it only reached 810 mm in Potrerillos and 678 mm in Huertitas. As already mentioned, data in Huertitas only covered 95% of the year, which may partially explain the lower volume recorded in this site. More generally, catchments located at higher elevations received larger precipitation amounts, probably because of orographic effects. The median rainfall intensities I_{50} recorded in 5 min throughout the rainy season differed among the sites: I_{50} amounted to 3.0 $mm.h^{-1}$ in Huertitas and La Cortina, and 4.8 $mm.h^{-1}$ in Potrerillos. In contrast, maximum intensities recorded were higher in Huertitas (118 $mm.h^{-1}$) and La Cortina (113 $mm.h^{-1}$) than in Potrerillos (72 $mm.h^{-1}$). Finally, in terms of kinetic energy release, La Cortina experienced more intense events (KE_{mm} [min-max]: [92-763] $J.m^{-2}.mm^{-1}$), which was explained by the generally higher volumes of rainfall characterizing this site. In

Huertitas and Potrerillos, KE_{mm} were lower and they remained in the same order of magnitude (respectively, [58-520] $J.m^{-2}.mm^{-1}$ and [42-463] $J.m^{-2}.mm^{-1}$).

3.1.2. Discharge and suspended sediment flux

The three subcatchments are characterized by very distinct hydrological behaviours: La Cortina hydrographs showed a high baseflow contribution to its total discharge (baseflow ranged between 0.01 and 0.1 $m^3.s^{-1}$, i.e., 0.05-0.15 m water depth); whereas in Huertitas, although the stream is perennial, baseflow was much lower ($< 1.10^{-3}$ $m^3.s^{-1}$ during the dry season, i.e., 0.01-0.05 m water depth). In Potrerillos, the water flow is ephemeral and characterized by successive flashflood events followed by fast recession times. According to historical records available at the outlet of the 630-km^2 basin, mean annual discharge during the period 1940-2002 was 2.3 $m^3.s^{-1}$. The mean discharge recorded during 2009 only reached 1.3 $m^3.s^{-1}$, which was the second lowest value in more than 60 years.

Hydrosedimentary patterns were also contrasted among the three study sites: La Cortina experienced relatively low SSC, even during storm events (SSC_{max} = 8 $g.l^{-1}$), whereas SSC peaks were much higher in Huertitas (SSC_{max} = 55 $g.l^{-1}$) and Potrerillos (SSC_{max} = 126 $g.l^{-1}$).

Two estimates of annual SSY were calculated in Huertitas and Potrerillos. This is the consequence of the incomplete sampling that occurred during the two major floods at both sites. Lower values correspond to a calculation that is strictly based on the data available, and upper values were estimated using the SSC peak estimations obtained for these two ungauged events (Table 3).

Overall, SSY were found to be subcatchment dependent, with high values in Huertitas ([900-1500] $t.km^{-2}.y^{-1}$) and Potrerillos ([600-800] $t.km^{-2}.y^{-1}$) contrasting with the > 20 times lower output recorded in La Cortina (30 $t.km^{-2}.y^{-1}$). Huertitas and Potrerillos showed a similar behaviour regarding sediment transport, and the slightly higher specific yield recorded in Huertitas could result from the greater extent of gullied areas (6% of the subcatchment area) generating high sediment inputs, as well as from steeper slopes (Table 1). In terms of loads exported during single events, the highest sediment bulk transport was measured in Potrerillos on 1 July 2009 (102 $t.km^{-2}$). The major event recorded in Huertitas generated 41 t of sediment km^{-2} on 26 June 2009. In La Cortina, it occurred on 14 July 2009 and reached 16 $t.km^{-2}$, contributing to half of the total load exported in 2009 from this subcatchment.

3.2. Analyzing suspended sediment dynamics

3.2.1. Hillslope particle detachment: comparison of rain intensity with SS loads

Both KE_{mm} and maximal intensities of each rainfall event were compared to SSC peaks. According to the two scatter plots presented in Fig. 3, each subcatchment followed a very distinct behaviour. Relatively random relationships were found between the tested parameters. High values of KE_{mm} were never associated with high SSC peaks (Fig. 3B). In all sites, maximal intensities showed slightly better correlations with sediment output values than KE_{mm} (Fig. 3A). In La Cortina and Huertitas, the heaviest storms were comparable in terms of intensity but the catchment responses were highly different: SSC peaks were much higher in Huertitas than in La Cortina (respectively, [3-55] $g.L^{-1}$ and [0.05-8] $g.L^{-1}$). Furthermore, significant SSC peaks were recorded in Potrerillos ([2-126] $g.L^{-1}$) despite lower maximum rainfall intensities.

3.2.2. SSC-discharge hysteretic patterns

The study sites are characterized by a remarkably fast runoff response to precipitation input (hydrograph rising phase < 5 min). A significant number of the storm events generated an “overflow wave” within channels that propagated down to the subcatchment outlet, inducing an instantaneous water level rise at the monitoring station. On such occasions we could not determine whether the sediment peak was leading the discharge peak or not. For that reason, the classical hysteresis typology had to be adapted (Fig. 4). These flash floods represented 35% of the events recorded in La Cortina in 2009, 54% in Potrerillos, and 69% in Huertitas. Such events were most likely due to the occurrence of Hortonian overland flow on surfaces characterized by a low permeability. Recession limbs were systematically more gradual.

Independent of location, a large majority of sedigraphs were found to maintain a high SSC level during the hydrograph recession phase. This characteristic was observed in 100% of events recorded in La Cortina, 100% in Huertitas, and 94% in Potrerillos. Consequently, the relation between SSC and discharge during the hydrograph falling stage could not be used as a discriminating factor. The classification was then adapted as follows:

(i) Lagging sediment peak events (referred to as “LaP” in Fig. 4): lag between the sediment peak and the discharge peak with sediment concentrations remaining at a high level during the recession phase. This situation corresponded to the absence of in-channel sediment delivery and to the arrival of remote sediment from external sources, i.e., hillslope erosion (Lenzi and Marchi, 2000; Orwin and Smart, 2004).

(ii) Simultaneous peak events (referred to as “SP” in Fig. 4): coincidence between sediment peak and peak discharge with sediment maintaining high concentrations during the recession phase.

(iii) Leading sediment peak events (referred to as “LeP” in Fig. 4): sediment peak leading discharge peak with sediment maintaining at a high level during recession. Both SP and LeP categories correspond to the remobilization and transport of in-channel sediments (Jansson, 2002; Smith and Dragovich, 2009) followed by a supply from distant sources (i.e., sediment still delivered during the falling phase). The possibility to discriminate between SP and LeP was conditioned by the non occurrence of “wave-type events.”

The classification of flood events through their hysteretic behaviour and their respective contribution to total sediment exports is summarized in Fig. 5. In La Cortina (Fig. 5A), the bulk of events exhibited a lagging SSC peak pattern, i.e., LaP events ($n = 14$). Two events were identified as SP, and LeP hysteresis was only observed once, during the event characterized by the highest peak discharge of the season. In Huertitas (Fig. 5B), events showing an LaP behaviour were also the most frequent ($n = 14$); a significant part of events exhibited SP hysteresis ($n = 7$), whereas during two events the sedigraph was leading (LeP). In contrast, in Potrerillos (Fig. 5C), the majority of events were SP ($n = 21$). Three events had an LeP pattern, whereas only five events were identified as LaP.

Apart from these site-specific responses, a general pattern was found among the three sites: SP and LeP events were clearly associated with high peak discharges and high SS loads, and with low to moderate rainfall intensities. Although these occurrences represented a minority of the sampled events, except in Potrerillos (average of 42%), they contributed significantly to the annual sediment export from the catchments (average of 70%; Fig. 5, small pie charts). In Potrerillos, 73% of SP and LeP events were preceded by high floods in the previous hours, as illustrated in Fig. 6. The first rainfall event began on 1 July 2009 at 4:30 p.m.; it resulted in a moderate catchment response governed by LaP dynamics (Fig. 6B). The following heavier storm generated a much higher sediment peak (SP event, Fig. 6C). In Huertitas, SP and LeP events were not systematically associated with high flood antecedents. Figure 7 shows an example of two successive stormflow events and illustrates another type of sediment dynamics. In that case, the catchment responded to a first precipitation input by a high discharge peak (SP event, Fig. 7B). The subsequent peak was much reduced in terms of fine sediment export, but the sediment response clearly led the peak discharge (LeP event, Fig. 7C). In La Cortina, no relationship was detected between flood antecedents and the type of SSC-Q relation.

3.2.3. Factorial analysis

The analysis in La Cortina was performed after having removed one outlier flood (corresponding to the major runoff event of the season). In each of the three sites, the most significant relationship was detected between SS load and Q_{max} (*RV* coefficients of 0.77 in La Cortina, 0.68 in Huertitas, and 0.46 in Potrerillos). In La Cortina, a positive correlation was also found, to a lesser extent though, between SSC peaks and Q_{max} (*RV* 0.48). Parameters associated with precipitation were absolutely not related to both sediment and discharge parameters. In Huertitas and Potrerillos, no other significant correlations were found. Overall, in the three sites, the statistical analysis underlined very weak correlations between rainfall parameters and sediment load.

3.2.4. Comparing peak discharges with SS loads

Given their good correlation, Q_{max} and SS load values were plotted on a single log-log graph (Fig. 8A). Scattering was high again, but we could identify significant trends. Each subcatchment had clearly a distinct hydrosedimentary behaviour. The higher erosion capacity observed in Potrerillos was confirmed. For equivalent peak discharges, specific loads were higher at this site than at both other stations. Huertitas also produced strong sediment exports whereas La Cortina experienced lower magnitude erosion processes.

The grain size distribution of sediment was also investigated (Fig. 8B). The grey triangle and the grey circle plotted in Fig. 8A correspond to events that occurred in Potrerillos and for which particle sizes are known (respectively, P1 and P2 in Fig 8B). Their distinct distribution on the diagram underlined the major dependence existing between the magnitude of storm events and the size of particles transported.

4. Discussion

4.1. Measurement uncertainties in responsive subcatchments

Only one event was missed during the 2009 rainy season in both Huertitas and Potrerillos. Those missing events introduced an uncertainty of ± 100 $t.km^{-2}.y^{-1}$ in Potrerillos (14% uncertainty) and of ± 300 $t.km^{-2}.y^{-1}$ in Huertitas (25% uncertainty). This underlines the strong difficulty to obtain accurate SSY estimates in such responsive subcatchments. It also confirms the observations made by other authors that the bulk of annual sediment export occurs during a single or a few high magnitude events (e.g., Walling and Webb, 1983; Mano et al., 2009; Navratil et al., 2009).

4.2. Which factors control the rates of erosion and sediment transport?

Splash erosivity was not a process driving sediment export (Fig. 3). Neither intensity nor overall energy of rainfall proved to be the main factor that triggered erosion processes at the catchment scale. The poor quality of the relationships can probably be explained by the high spatial variability of rainfall. Borga et al. (2008) recently pointed out that flash flood monitoring requires rainfall estimates at spatial scales of 1 km or even finer; such requirements can be met for instance by using weather radar networks.

The effects of vegetation on sediment erosion within hillslopes have also probably affected the rainfall/sediment relationship in different ways.

Hysteretic pattern analysis was interpreted as a descriptor of the local conditions existing close to the gauging stations rather than a hydrosedimentary behaviour affecting the entire surface of the subcatchments. At a local scale, sediment stock appeared to be limited in Huertitas and La Cortina (majority of LaP events, Fig. 5). This was probably because of the locally incised morphology of those two subcatchments, with accelerated flow preventing the local deposition of sediment within the channels. We could not identify any sediment exhaustion effect. In Potrerillos, sediment stored in the channel seemed to be locally continuously available, as demonstrated by a majority of SP events and a higher amount of LeP events (Fig. 5). Distant sediment sources were also active as no early sediment depletion was observed. These observations match with results obtained in 2008 from scour chain surveys (unpublished data; see the methodology described by Laronne et al., 1994), which indicated a succession of scouring and deposition phases within the channel close to the gauging station in Potrerillos.

However, at the subcatchment scale, temporary in-channel sediment storage was evidenced in the three sites. This is confirmed by the occurrence of SP and LeP events and by their highly significant contribution to the sediment export from all the stations (Fig. 5). River networks and the connected gullies thus acted as very responsive compartments characterized by successive phases of sediment storage and sediment flush.

The succession of storms appeared to play a controlling role on generation of SP and LeP events in most cases in Potrerillos and in a few cases in Huertitas. This “memory effect” has already been documented by Jansson (2002) and Sayer et al. (2006). In Fig. 6, the first event (LaP) is thought to have provided a refilling of the channel storage. The following storm gave rise to a SP event because of the remobilization of sediment previously deposited within the channel (i.e., channel flush). All SSC recorded during the falling limb of this second event reached particularly high values compared to their associated discharges, already at recession level (e.g., last sample collected at 8:10 p.m.: SSC reached 63 $g.L^{-1}$ for a discharge of 0.46 $m^3.s^{-1}$). This probably indicates that channels were transport-limited during recession. This argument is further discussed in section 4.3.

In Fig. 7, the first event (SP) allowed a direct transit of sediments from eroded hillslopes down to the subcatchment outlet. The subsequent sediment peak (LeP) probably illustrates the resuspension of the small quantities of in-channel sediment deposited during the preceding event; the lower SSC peak value was attributed to a pronounced exhaustion of sediment available in the network (i.e., because of the high magnitude of the previous event). Again, recession was concomitant with an external sediment contribution from hillslopes (transport-limited state). This is consistent with results reported by Evrard et al. (in review), which indicated that the proportion of new sediment in the river channel decreased from ca. 100% to 20% after this event.

Overall, the study of sediment dynamics through hysteretic behaviour allowed explanation, to a certain extent, of the processes occurring at the subcatchment scale. Our results show that previous floods had an influence on sediment delivery, which can be explained by an increase in hillslope–channel connectivity when moisture conditions increased and when high quantities of sediment were available.

The study of the relationship between peak discharges and SS loads (Fig. 8A) confirmed that each subcatchment followed a specific hydrosedimentary behaviour. The potential bias implied by the comparison of some instantaneous values (i.e., Q_{max}) with integrated ones (i.e., SS load) was most likely offset by the fact that, in these small subcatchments, Q_{max} acted as a parameter integrating both rainfall and runoff features.

Huertitas and Potrerillos subcatchments experienced a higher vulnerability to erosion and a higher reactivity to storms, whereas sediment was exported at a lower rate from La Cortina. In Cointzio, the presence of gullied areas in subcatchments proved to play a significant role in fine sediment erosion. In the first two subcatchments, historical gullies provided a constant sediment supply to the river. One of the primary factors that constrained suspended sediment delivery to outlets was therefore sediment availability. Dense networks of historical gullies certainly increased the catchment connectivity, as already reported by Tamene et al. (2006). Two other key factors were the steepness of hillslopes and the proportion of cropland and rangeland within the subcatchments; both factors being higher in Huertitas and Potrerillos than in La Cortina. Bravo-Espinosa et al. (2009) recently established that the association of traditional cropping practices with cattle grazing could lead to severe soil degradation in the Cointzio basin. We can therefore hypothesize that the formation of gullies in Huertitas and Potrerillos was triggered by those practices.

Overall, land degradation associated with historical human disturbance has been widely recognized as a major driver of soil erosion in Mexico (e.g., Alcántara-Ayala et al., 2006; Cotler and Ortega-Larrocea, 2006; Geissen et al., 2009).This linkage between human-induced land use changes and soil degradation was also reported from numerous other areas of the world (e.g., Wasson et al., 1998, in Australia; Zhang et al., 2004, in China; Kasai et al., 2005, in New-Zealand; Valentin et al., 2008, in south-eastern Asia).

4.3. In-channel transport processes

Sediment export systematically increased with discharge (Fig. 8A). This process was observed across the three sites. Consequently, the limiting factor at the subcatchment scale was probably not the sediment availability. If that had been the case, a threshold would have been observed in SS load values. As sediment transport was not limited by sediment availability, the in-channel transport capacity appeared to be a driving factor controlling the suspended sediment export rate. From a physical point of view, the sediment transport capacity of a stream is directly related to flow velocity and to the settling velocity of the particles transported (Engelund and Hansen, 1967; Dietrich, 1982). According to Stokes' law (Batchelor, 1967), a strong relationship exists between the diameter of a particle and its settling velocity:

$$w_s \propto D^2 \tag{3}$$

where w_s is the settling velocity of a spherical particle (m.s^{-1}), and D is its diameter (m). Particle diameter can thus reasonably be considered as a good proxy for estimating its settling velocity. In an exploratory approach, study of grain size distribution of sediment was performed for each site on individual floods. As shown in Fig. 8B, particle sizes were very heterogeneous even within a single subcatchment, as suggested by the values measured during two distinct events in Potrerillos (event 1: median diameter D_{50} = 24 µm; event 2: D_{50} = 6 µm). Interstorm variability was even higher than intersite variability. Grain size estimates in each subcatchment would thus require a complete granulometric study that is beyond the scope of this paper. Flow discharge was therefore conserved as an indirect indicator for the upward vertical turbulent velocity, whereas SSC was considered as a broad indicator for the sediment settling flux (higher SSC requiring higher energy to be transported).

A study of the relationship between SSC and Q was carried out in order to identify to what extent the two parameters were associated and whether some subpatterns could be identified from the available time series (Fig. 9). Among all SSC-Q data collected in 2009, values derived from the falling stages of the hydrographs were of particular interest. While water flow was decreasing, high SSC values were indeed frequently measured because of the severe hysteretic pattern generally observed. Such behaviour was already deduced from the temporal analysis presented in section 4.2 and Fig. 6. The limit in stream transport capacity should have been reached in such circumstances. Figure 9 displays all SSC-Q values recorded during the 2009 rainy season. It differentiates values occurring at falling stage from the others.

Independently of the location, the points recorded during recession phases were located in the upper part of the scatter plots. In Potrerillos (Fig. 9A), these highest values as well as a few others clearly defined an upper boundary that very likely corresponds to the limit of stream transport capacity. The direct consequence of reaching this physical constraint was the generation of a net sediment deposition in the channel (Jansson, 2002). This hypothesis supports the visual observations made in the field all throughout the season. Erosive power of the stream was outlined by minimal values of detachment capacity (lower boundary). This limit was approximately delineated, even though the presence of two outliers can put its relevance into question (Fig. 9A).

In Huertitas (Fig. 9B) an upper boundary was also detected. Again, it was associated with the in-channel transport capacity. The stream ability to erode and export sediment was also clearly outlined: the lower boundary in Fig. 9B corresponds to the minimum sediment load that the stream was able to dislodge from the riverbed. This finding supports the results of section 4.2 that outlined that little material was stored within the channel and that the streambed was preferentially eroded.

In La Cortina (Fig. 9C), both boundaries were also outlined, but the transport capacity was much lower than in the two other sites. Again, this was consistent with findings of section 4.2 (little sediment stored locally). Because of the relatively limited sediment supply, the streambed is probably affected almost permanently by erosive conditions; the highly incised morphology of the river channel in La Cortina could be a consequence of this situation.

All the values defining the upper and lower limits were associated with distinct storm events; it proves that a general behaviour was identified rather than transitory conditions prevailing during a specific flood.

4.4. Seasonality in sediment delivery

Figure 10 shows the evolution of SSC values during the rainy season calculated for each storm event. Despite a strong dispersion, mean SSC time series exhibited a decreasing trend in all the subcatchments (Fig. 10A). Furthermore, this seasonal effect was neither related to a change in peak discharges nor to a change in rainfall regime. This evolution throughout the rainy season was even clearer in La Cortina and Huertitas. It probably illustrates the progressive increase in the soil cover by vegetation in these partly cultivated hillslopes (see Table 1), which is known to protect the soil against the erosive action of rainfall. Similarly, sediment exported from Huertitas may not exclusively originate from bare gullies (Evrard et al., in review).

In Huertitas, the highest mean SSC values were observed at the beginning of the wet season (60 $kg.m^{-3}$ on 15 May 2009). In Potrerillos and La Cortina, the most erosive events occurred during the first part of the rainy season (respectively, 101 $kg.m^{-3}$ on 1 July 2009 and 3 $kg.m^{-3}$ on 14 July 2009). This outlines a progressive flush of the channel sediment stock at the beginning of the rainy season (Hudson, 2003; Evrard et al., in review).

Furthermore, a change was identified in La Cortina and Huertitas SSC records. SSC values experienced a significant decrease even when associated with high discharge peaks. This change affected all SSC data collected, as shown in Figs. 10B and 10C. At both sites, SSC decrease was linked with an increase in baseflow contribution and occurred from 3 August 2009 in La Cortina (Fig. 10B) and from 4 September 2009 in Huertitas (Fig. 10C). Again, this remarkable change of the hydrosedimentary processes probably illustrates the impact of land cover change through the rainy season.

4.5. Comparison with other subcatchment sediment yields reported in the world

We aimed at comparing our results to previous research carried out in small catchments (1-10 km^2). However, most of the references found in the literature report measurements in mesoscale to large basins (i.e., > 100 km^2). According to the few data available for comparison, sediment export in La Cortina appeared to be low to moderate (Table 4); it roughly corresponds to values measured in lowland areas under temperate climate (Walling et al., 2002; Goodwin et al., 2003; Lefrançois et al., 2007; Smith, 2008). SSY estimates in Huertitas and Potrerillos were much higher, and they can be compared to the loads exported from a mountainous subcatchment located in the northern Ethiopian Highlands (Nyssen et al., 2008). However, sediment exports in Potrerillos and Huertitas remain lower than export rates measured by Mathys et al. (2003) in highly erodible marly terrains of the French Alps. Nevertheless, we hypothesized that the values we found are representative of upstream catchments locally undergoing severe erosion processes. Overall, our results provide very useful erosion estimates for small mountainous catchments with a subhumid climate, which remain largely undocumented in the literature.

5. Conclusions

For the first time, suspended sediment yields of three upland subcatchments located in the Mexican Central Highlands were estimated during a whole year. Each subcatchment exhibited a specific behaviour. Two catchments exported high sediment yields (i.e., Huertitas, [900-1500] $t.km^{-2}.y^{-1}$ and Potrerillos, [600-800] $t.km^{-2}.y^{-1}$). In contrast, the third catchment generated a rather low sediment export (i.e., La Cortina, 30 $t.km^{-2}.y^{-1}$). At the scale of the entire 630-km^2 basin, we could not derive any direct relationship between rainfall intensity and sediment concentration. This can be explained by the high spatial variability of rainfall and by the effect of the vegetation growth throughout the season, which provided a protection to the soil against erosive rainfall. Erodible sediment availability on hillslopes was identified as the main factor controlling suspended sediment delivery. The occurrences of numerous active gullies in Huertitas and Potrerillos provided a constant sediment source linked to the river network, which explains the high SSY recorded at both stations. At the subcatchment scale, a combination of various parameters was responsible for sediment control. Peak discharges during floods were found to be significantly associated with exported loads; discharge proved to be a controlling factor when sediment was not lacking. This limit in stream transport capacity preferentially occurred during hydrograph falling limbs. A minimum erosive power was detected in Huertitas and La Cortina. It was regularly reached during floods. In these subcatchments, the role of seasonality was particularly clear, with higher sediment export in the first months of the rainy season. This may be attributed to the growth of the vegetation throughout the rainy season. The rapid succession of several storms was also a cause for high sediment exports, and particularly in Potrerillos. This was associated with a preliminary filling of the channel storage, without compaction or drying out of particles, which was rapidly followed by a channel flush; but it may also be due to a better connectivity between active gullies and stream channels.

Further studies should now concentrate on a better characterization of fine sediment settling flux within channels in order to improve our physical understanding of deposition/resuspension dynamics at the subcatchment scale. Furthermore, the study of nested subcatchments at the scale of the entire Cointzio basin should be carried out. It would provide useful information on suspended sediment behaviour across mesoscale river basins and contribute to improve hydrosedimentary models.

Acknowledgements

This is the LSCE contribution n°4342. This work was supported by the STREAMS project (*Sediment TRansport and Erosion Across MountainS*), funded by the French National Research Agency, as well as by the DESIRE project (*Desertification mitigation and remediation of land*), funded by the European Union. The authors would like to acknowledge the CIGA-UNAM, especially Gerardo Bocco, Manuel Mendoza-Cantú, Hilda Rivas-Solórzano, and Rosaura Páez-Bistrain, for kindly giving us access to their laboratory facilities and for allowing us to work in pleasant conditions. We also wish to thank Roberto Anguiano-Valencia and Arely Vazquez-Ramirez for their assistance with rainfall data collection and laboratory work, and all the local staff for their help with field sample collection. Finally, we are grateful to Dr. Richard A. Marston and to four anonymous referees whose comments helped us improve the quality of this manuscript.

References

Alcántara-Ayala, I., Esteban-Chávez, O., Parrot, J.F., 2006. Landsliding related to land-cover change: a diachronic analysis of hillslope instability distribution in the Sierra Norte, Puebla, Mexico. Catena 65, 152–165.

Alcocer, J., Escobar, E., 1993. Morphometric characteristics of six Mexican coastal-lakes related to productivity. Rev. Biol. Trop. 41 (2), 171–179.

Anguiano-Valencia, R., 2010. Informe del monitoreo pluviográfico de la cuenca de Cointzio. Universidad Michoacana de San Nicolás de Hidalgo, Institut de Recherche pour le Développement, Morelia, Mexico, 36 pp.

Asselman, N.E.M., 1999. Suspended sediment dynamics in a large drainage basin: the River Rhine. Hydrol. Process. 13, 1437–1450.

Batchelor, G.K., 1967. An Introduction to Fluid Dynamics. Cambridge University Press, 1st edition, Cambridge, UK, 615 pp.

Borga, M., Gaume, E., Creutin, J.D., Marchi, L., 2008. Surveying flash flood response: gauging the ungauged extremes. Hydrol. Process. 22 (18), 3883–3885.

Brandt, C.J., 1990. Simulation of the size distribution and erosivity of raindrops and throughfall drops. Earth Surf. Proc. Land. 15, 687–698.

Bravo-Espinosa, M., Mendoza, M.E., Medina-Orozco, L., Prat, C., García-Oliva, F., López-Granados, E., 2009. Runoff, soil loss, and nutrient depletion under traditional and alternative cropping systems. Land Degrad. Dev. 20 (6), 640–653.

Carlón-Allende, T., Mendoza, M.E., López-Granados, E.M., Morales-Manilla, L.M., 2009. Hydrogeographical regionalization: an approach for evaluating the effects of land cover change in watersheds, a case study in the Cuitzeo lake watershed, central Mexico. Water Resour. Manag. 23 (12), 2587–2603.

Chappell, N.A., McKenna, P., Bidin, K., Douglas, I., Walsh, R.P.D., 1999. Parsimonious modelling of water and suspended-sediment flux from nested-catchments affected by selective tropical forestry. Phil. Trans. Roy. Soc. Lond. 354, 1831–1846.

Cotler, H., Ortega-Larrocea, M.P., 2006. Effects of land use on soil erosion in a tropical dry forest ecosystem, Chamela watershed, Mexico. Catena 65, 107–117.

Descroix, L., González-Barrios, J.L., Viramontes, D., Poulenard, J., Anaya, E., Esteves, M., Estrada, J., 2008. Gully and sheet erosion on subtropical mountain slopes: their respective roles and the scale effect. Catena 72, 325–339.

Dietrich, W.E., 1982. Settling velocity of natural particles. Water Resour. Res. 18 (6), 1615–1626.

Dietrich, W.E., Dunne, T., 1978. Sediment budget for a small catchment in mountainous terrain. Zeits. Geomorph. 29, 191–206.

Duvert, C., 2009. Stage-discharge Rating Curves Construction in Huertitas, La Cortina and Potrerillos – Associated Uncertainties. Technical report, Institut de Recherche pour le Développement, Morelia, Mexico, 6 pp.

Engelund, F., Hansen, E., 1967. A Monograph on Sediment Transport in Alluvial Streams. Teknisk Forlag, Copenhagen, Denmark.

Escoufier, B., 1979. Traitement simultané de variables quantitatives et qualitatives en analyse factorielle. Les cahiers de l’analyse des données 4 (2), 137–146.

European ISO EN Rule 748, 1997. Measurement of Liquid Flow in Open Channels – Velocity-area Methods. Reference number ISO 748:1997 (E), International Standard, International Organization for Standardization, Geneva, Switzerland.

Evrard, O., Némery, J., Gratiot, N., Duvert, C., Ayrault, S., Lefèvre, I., Poulenard, J., Prat, C., Bonté, P., Esteves, M., in review. Sediment dynamics during the rainy season in tropical highland catchments of central Mexico using fallout radionuclides. Geomorphology.

Food and Agriculture Organization of the United Nations (FAO), 2006. World Reference Base for Soil Resources 2006, A Framework for International Classification, Correlation and Communication. World Soil Resources Report 103, FAO, Rome, Italy.

Fryirs, K., Brierley, G.J., 1999. Slope-channel decoupling in Wolumla catchment, New South Wales, Australia: the changing nature of sediment sources following European settlement. Catena 35, 41–63.

Gao, P., 2008. Understanding watershed suspended sediment transport. Prog. Phys. Geog. 32, 243–263.

Geissen, V., Sánchez-Hernández, R., Kampichler, C., Ramos-Reyes, R., Sepulveda-Lozada, A., Ochoa-Goana, S., Jong, B.H.J., Huerta-Lwanga, E., Hernández-Daumas, S., 2009. Effects of land-use change on some properties of tropical soils – an example from Southeast Mexico. Geoderma 151, 87–97.

Gomi, T., Moore, R.D., Hassan, M., 2005. Suspended sediment dynamics in small forested streams of the Pacific Northwest. J. Am. Water Resour. Assoc. 41 (4), 877–898.

Goodwin, T.H., Young, A.R., Holmes, G.R., Old, G.H., Hewitt, N., Leeks, G.J.L., Packman, J.C., Smith, B.P.G., 2003. The temporal and spatial variability of sediment transport and yields within the Bradford Beck catchment, West Yorkshire. Sci. Total Environ. 314–316, 475–494.

Gratiot, N., Duvert, C., Collet, L., Vinson, D., Némery, J., Sáenz-Romero, C., 2010. Increase in surface runoff in the central mountains of Mexico: lessons from the past and predictive scenario for the next century. Hydrol. Earth Syst. Sci. 14, 291–300.

Hudson, P.F., 2003. Event sequence and sediment exhaustion in the lower Panuco basin, Mexico. Catena 52, 57–76.

Instituto Nacional de Estadística y Geografía (INEGI), 2006. Conteo de Población y Vivienda 2005, Resultados definitivos. Sistema Nacional de Información Estadística y Geográfica, Mexico City, Mexico.

Jansson, M.B., 2002. Determining sediment source areas in a tropical river basin, Costa Rica. Catena 47, 63–84.

Jeje, L.K., Ogunkoya, O.O., Oluwatimilehin, J.M., 1991. Variation in suspended sediment concentration during storm discharges in three small streams in upper Osun Basin, central western Nigeria. Hydrol. Process. 54, 361–369.

Kasai, M., Brierly, G.J., Page, M.J., Marutani, T., Trustrum, N.A., 2005. Impacts of land use change on patterns of sediment flux in Weraamaia catchment, New Zealand. Catena 64 (1), 27–60.

Klein, M., 1984. Anti clockwise hysteresis in suspended sediment concentration during individual storms. Catena 11, 251–257.

Lang, A., Bork, H.R., Mäckel, R., Preston, N., Wunderlich, J., Dikau, R., 2003. Changes in sediment flux and storage within a fluvial system — some examples from the Rhine catchment. Hydrol. Process. 17, 3321–3334.

Laronne, J.B., Outhet, D.N., Carling, P.A., McCabe, T.J., 1994. Scour chain employment in gravel bed rivers. Catena 22, 299–306.

Lê, S., Josse, J., Husson, F., 2008. FactoMineR: an R package for multivariate analysis. J. Stat. Softw. 25 (1), 1–18.

Lefrançois, J., Grimaldi, C., Gascuel-Odoux, C., Gilliet, N., 2007. Suspended sediment and discharge relationships to identify bank degradation as a main sediment source on small agricultural catchments. Hydrol. Process. 21, 2923–2933.

Lenzi, M.A, Marchi, L., 2000. Suspended sediment load during floods in a small stream of the Dolomites (northeastern Italy). Catena 39, 267–282.

López-Tarazón, J.A., Batalla, R.J., Vericat, D., Francke, T., 2009. Suspended sediment in a highly erodible catchment: the River Isábena (southern Pyrenees). Geomorphology 109, 210–221.

Mano, V., Némery, J., Belleudy, P., Poirel, A., 2009. Suspended particle matter dynamics in four Alpine watersheds (France): influence of climatic regime and optimization of flux calculation. Hydrol. Process. 23, 777–792.

Mathys, N., Brochot, S., Meunier, M., Richard, D., 2003. Erosion quantification in the small marly experimental catchments of Draix (Alpes de Haute Provence, France). Calibration of the ETC rainfall–runoff–erosion model. Catena 50, 527–548.

Nadal-Romero, E., Latron, J., Martí-Bono, C, Regüés, D., 2008. Temporal distribution of suspended sediment transport in a humid Mediterranean badland area: the Araguás catchment, central Pyrenees. Geomorphology 97, 601–616.

Navratil, O., Esteves, M., Némery, J., Legout, C., Poirel, A., Gratiot, N., Belleudy, P., 2009. Uncertainties and Spatiotemporal Variations of Suspended Sediment Flux in the Bleone River Basin (Southern French Alps). EGU General Assembly 2009, Vienna, Austria.

Newcombe, C.P., McDonald, D.D., 1991. Effects of suspended sediments on aquatic ecosystems. N. Am. J. Fish. Manag. 11, 72–82.

Nyssen, J., Poesen, J., Moeyersons, J., Mitiku, H., Deckers, J., 2008. Dynamics of soil erosion rates and controlling factors in the Northern Ethiopian highlands – towards a sediment budget. Earth Surf. Proc. Land. 33 (5), 695–711.

Oeurng, C., Sauvage, S., Sánchez-Pérez, J.M., 2010. Dynamics of suspended sediment transport and yield in a large agricultural catchment, southwest France. Earth Surf. Proc. Land. DOI: 10.1002/esp.1971.

Ongley, E.D., 1996. Control of Water Pollution from Agriculture. Irrigation and Drainage Paper 55, FAO, Rome, Italy, 101 pp.

Orwin, J.F., Smart, C.C., 2004. The evidence for paraglacial sedimentation and its temporal scale in the deglacierizing basin of Small River Glacier, Canada. Geomorphology 58, 175–202.

Owens, P.N., Batalla, R.J., Collins, A.J., Gomez, B., Hicks, D.M., Horowitz, A.J., Kondolf, G.M.., Marden, M., Page, M.J., Peacock, D.H., Petticrew, E.L., Salomons, W., Trustrum, N.A., 2005. Fine-grained sediment in river systems: environmental significance and management issues. River Res. Applic. 21, 693–717.

Pagès, J., 2004. Analyse factorielle de données mixtes. Rev. Statistique Appliquée 52 (4), 93–111.

Pimentel, D., Harvey, C., Resosudarmo, P., Sinclair, K., Kurz, D., McNair, M., Crist, S., Sphpritz, L., Fitton, L., Saffouri, R., Blair, R., 1995. Environmental and economic costs of soil erosion and conservation benefits. Science 267, 1117–1123.

Poesen, J., 1985. An improved splash transport model. Zeits. Geomorph. 29, 193–211.

Poulenard, J., Podwojewski, P., Janeau, J.L., Collinet, J., 2001. Runoff and soil erosion under rainfall simulation of Andisols from the Ecuadorian Páramo: effect of tillage and burning. Catena 45, 185–207.

Quansah, C., 1981. The effect of soil type, slope, rain intensity and their interactions on splash detachment and transport. J. Soil Science 32, 215–224.

Ramírez-León, J.M., Aparicio, J., 2009. Estimation of sediment yield in watersheds. Application to the Apulco River, Mexico. Ing. Hidraul. Mex. 24 (4), 145–157.

Robert, P., Escoufier, Y., 1976. A unifying tool for linear multivariate statistical methods: the RV-coefficient. Applied Statistics 25 (3), 257–265.

Sadeghi, S.H.R., Mizuyama, T., Miyata, S., Gomi, T., Kosugi, K., Fukushima, T., Mizugaki, S., Onda, Y., 2008. Determinant factors of sediment graphs and rating loops in a reforested watershed. J. Hydrol. 356, 271–282.

Salles, C., Poesen, J., Sempere-Torres, D., 2002. Kinetic energy of rain and its functional relationship with intensity. J. Hydrol. 257, 256–270.

Sayer, A.M., Walsh, R.P.D., Bidin, K., 2006. Pipeflow suspended sediment dynamics and their contribution to stream sediment budgets in small rainforest catchments, Sabah, Malaysia. Forest Ecol. Manag. 224, 119–130.

Secretaría de Medio Ambiente y Recursos Naturales (SEMARNAT), Colegio de Postgraduados (CP), 2003. Evaluación de la Degradación del Suelo Causada por el Hombre en la República Mexicana. Escala 1:250000. Memoria Nacional 2001-2002, Mexico City, Mexico.

Seeger, M., Errea, M.P., Begueria, S., Arnaez, J., Marti, C., García-Ruiz, J.M., 2004. Catchment soil moisture and rainfall characteristics as determinant factors for discharge/suspended sediment hysteretic loops in a small headwater catchment in the Spanish Pyrenees. J. Hydrol. 288, 299–311.

Servenay, A., Prat, C., 2003. Erosion extension of indurated volcanic soils of Mexico by aerial photographs and remote sensing analysis. Geoderma 117, 367–375.

Sidle, R.C., Tsuboyama, Y., Noguchi, S., Hosoda, I., Fujieda, M., Shimizu, T., 2000. Stormflow generation in steep forested headwaters: a linked hydrogeomorphic paradigm. Hydrol. Process. 14, 369–385.

Smith, H.G., 2008. Estimation of suspended sediment loads and delivery in an incised upland headwater catchment, south-eastern Australia. Hydrol. Process. 22, 3135–3148.

Smith, H.G., Dragovich, D., 2009. Interpretation of sediment delivery processes using suspended sediment-discharge hysteresis patterns from nested upland catchments, south-eastern Australia. Hydrol. Process. 23, 2415-2426.

Susperregui, A.S., Gratiot, N., Esteves, M. Prat, C., 2009. A preliminary hydrosedimentary view of a highly turbid, tropical, manmade lake: Cointzio Reservoir (Michoacán, Mexico). Lakes & Reservoirs Research and Management 14 (1), 31–39.

Tamene, L., Park, S.J., Dikau, R., Vlek, P.L.G., 2006. Analysis of factors determining sediment yield variability in the highlands of northern Ethiopia. Geomorphology 76, 76–91.

Valentin, C., Agus, F., Alamban, R., Boosaner, A., Bricquet, J.P., Chaplot, V., de Guzman, T., de Rouw, A., Janeau, J.L., Orange, D., Phachomphonh, K., Phai, D., Podwojewski, P., Ribolzi, O., Silvera, N., Subagyono, K., Thiébaux, J.P., Tran Duc T., Vadari, T., 2008. Runoff and sediment losses from 27 upland catchments in southeast Asia: impact of rapid land use changes and conservation practices. Agric. Ecosyst. Environ. 128, 225–238.

Vidal, J., Valero, M., Rangel, R., 1985. Frontera acuícola. Comisión del Plan Nacional Hidráulico, Mexico City, Mexico, 216 pp.

Viramontes, D., Esteves, M., Descroix, L., Duwig, C., Rojas-Rojas, F., Gutiérrez, A., de León-Mojarro, B., 2008. Quantification of runoff and erosion in an experimental Andosol watershed in Valle de Bravo. Ing. Hidraul. Mex. 23 (3), 89-103.

Walling, D.E., Webb, B.W., 1983. Patterns of sediment yield. In: Gregory, K.J. (Ed.), Background to Paleohydrology. Wiley, New York, NY, pp. 69–100.

Walling, D.E., Webb, B.W., 1996. Erosion and sediment yield, a global overview. In: Walling, D.E., Webb, B.W. (Ed.), Erosion and Sediment Yield: Global and Regional Perspectives. Proceedings of the Exeter Symposium, Jul 1996, IAHS Publication 236, Wallingford, UK, pp. 3–19.

Walling, D.E., Russell, M.A., Hodgkinson, R.A., Zhang, Y., 2002. Establishing sediment budgets for two small lowland agricultural catchments in the UK. Catena 47, 323–353.

Wasson, R.J., Mazari, R.K., Starr, B., Clifton, G., 1998. The recent history of erosion and sedimentation on the Southern Tablelands of southeastern Australia: sediment flux dominated by channel incision. Geomorphology 24, 291–308.

Webb, B.W., Walling, D.E., 1982. The magnitude and frequency characteristics of fluvial transport in a Devon drainage basin and some geomorphological implications. Catena 9, 9–23.

Williams, G.P., 1989. Sediment concentration versus water discharge during single hydrologic events in rivers. J. Hydrol. 111, 89–106.

Zabaleta, A., Martínez, M., Uriarte, J.A., Antigüedad, I., 2007. Factors controlling suspended sediment yield during runoff events in small headwater catchments of the Basque country. Catena 71 (1), 179–190.

Zhang, B., Yang, Y., Zepp, H., 2004. Effect of vegetation restoration on soil and water erosion and nutrient losses of a severely eroded clayey Plinthudult in southeastern China. Catena 57, 77–90.

List of Figures

Fig. 1. Location of the study sites.

Fig. 2. Partial view of the succession of cropland, rangeland, and gully networks in the Huertitas subcatchment (the photograph was taken by J. Poulenard in July 2009).

Fig. 3. Scatter plot of sediment peak and rainfall characteristics for each site and for each event of the 2009 rainy season. (A) Maximal intensity versus SSC peak; (B) kinetic energy versus SSC peak.

Fig. 4. Revision of the typology proposed by Williams (1989) to classify SSC-discharge hysteresis patterns. In case of flash flood events (instantaneous water level rise, representing 50% of total events), the classification of Williams (1989) (left) does not allow a proper differentiation between these different situations given that all events would be characterized by a counterclockwise loop. The adapted version (right) proposes to classify the events as showing a sediment peak lagging (LaP), simultaneous peaks (but still with counterclockwise pattern, SP), or a sediment peak leading (LeP).

Fig. 5. Repartition of runoff events between the three types of hysteresis patterns determined in Fig. 4. The large pie charts refer to the relative importance of SP (i.e., simultaneous SSC and *Q* peaks) and LeP (i.e., sediment peak leading) events (in black) compared to the total amount of events recorded during the season. The small pie charts refer to the contribution of SP and LeP events (in black) to the total sediment export. “Und.” refers to unclassified events.

Fig. 6. Multipeak event recorded in Potrerillos on 1 July 2009: (A) series of precipitation, discharge, and SSC; (B) representation of SSC-Q hysteresis of the first flood peak; (C) representation of SSC-Q hysteresis of the second flood peak. Grey bars correspond to a 20% mean-centered error.

Fig. 7. Multipeak event recorded in Huertitas on 4 September 2009: (A) series of precipitation, discharge, and SSC; (B) representation of SSC-Q hysteresis of the first flood peak; (C) representation of SSC-Q hysteresis of the second flood peak. Grey bars correspond to a 20% mean-centered error.

Fig. 8. (A) Relationship between specific SSL and specific discharge peak (Q_{max}), taking into account each rainfall–runoff event that occurred in the three sites all throughout the rainy season. The grey triangle refers to Potrerillos data and stands for the 19 July 2009 event, corresponding to P1 in (B); the grey circle also refers to Potrerillos data and stands for the 23 July event, corresponding to P2 in (B). Error bars were associated with extreme values in each site; they correspond to a 30% error on SSL estimate. (B) Grain size distributions of four sediment samples collected during different stormflow events. P1 and P2 refer to sediment collected in Potrerillos, respectively, on 19 July and 23 July 2009; H refers to sediment collected in Huertitas on 12 July 2009; C refers to sediment collected in La Cortina on 14 July 2009.

Fig. 9. SSC-Q values obtained from data collected all throughout the 2009 rainy season. Black squares correspond to SSC-Q data recorded during hydrograph recession phases, and grey squares correspond to all remaining data.

Fig. 10. Seasonality effects on sediment delivery rates: (A) mean SSC per event throughout the season for the three subcatchments. A threshold can be identified in values recorded in both La Cortina and Huertitas, corresponding to a sharp decrease in sediment export. Transitions are defined by black bars: (B) in La Cortina, the transition from white to grey squares occurred on 3 August 2009; (C) in Huertitas, the transition from white to grey circles occurred on 4 September 2009.

Fig. 1

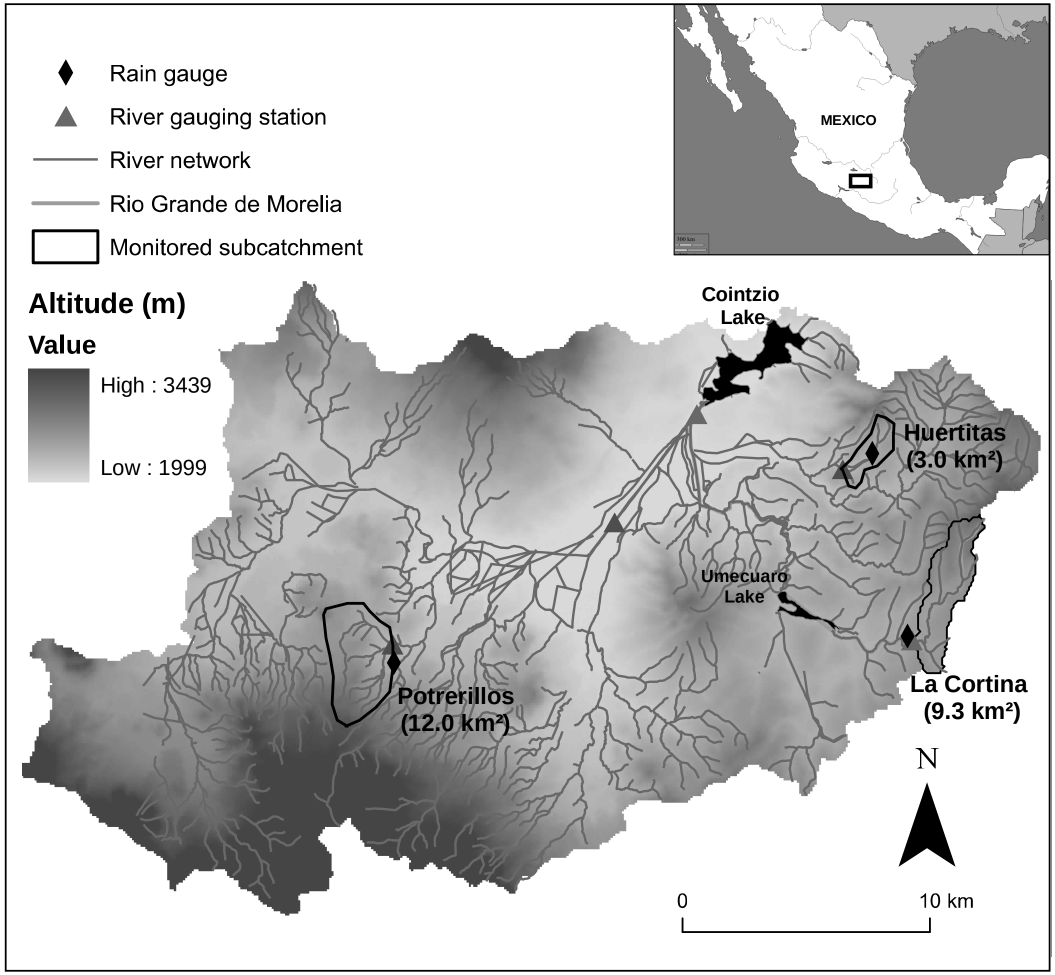
Rain gauge
River gauging station
River network
Rio Grande de Morelia
Monitored subcatchment
MEXICO
Altitude (m)
Value
High : 3439
Low : 1999
Cointzio Lake
Huertitas (3.0 km²)
Umecuaro Lake
Potrerillos (12.0 km²)
La Cortina (9.3 km²)
N
0
10 km

Fig. 2

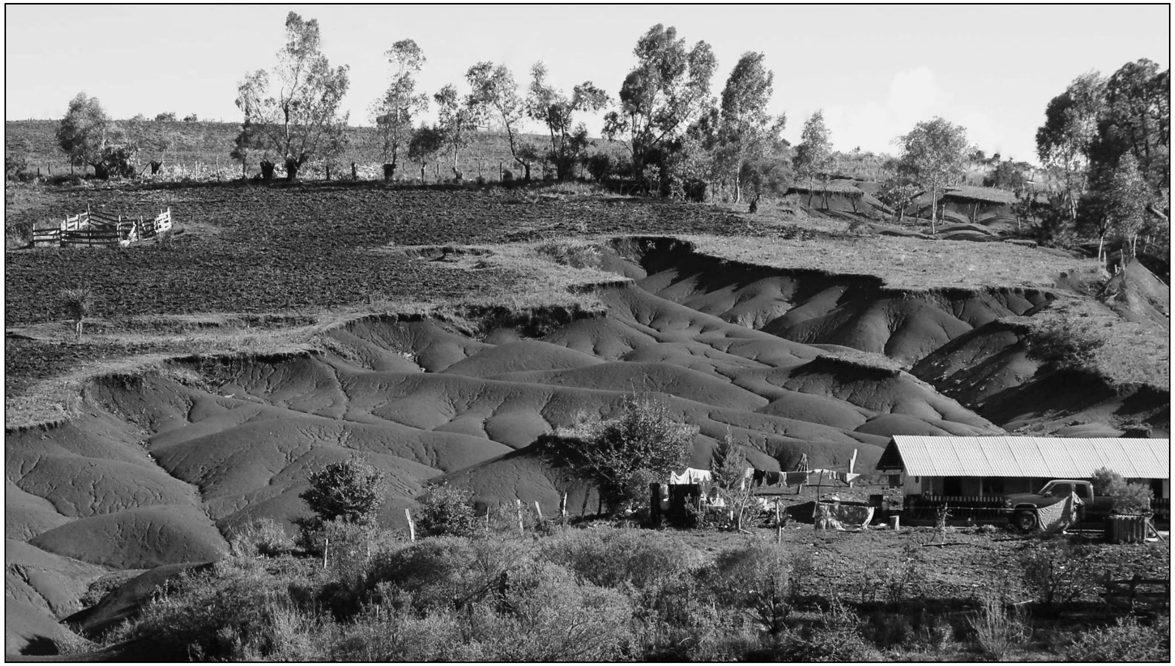

Fig. 3

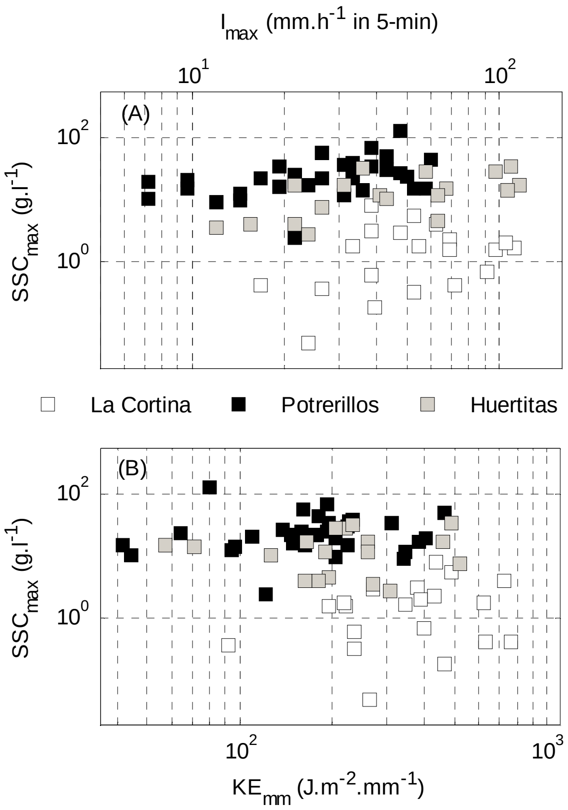

I_{max} (mm.h^{-1} in 5-min)
10^1
10^2
(A)
10^2
10^0
SSC_{max} (g.l^{-1})
La Cortina
Potrerillos
Huertitas
(B)
10^2
10^0
SSC_{max} (g.l^{-1})
10^2
10^3
KE_{mm} (J.m^{-2}.mm^{-1})

Fig. 4

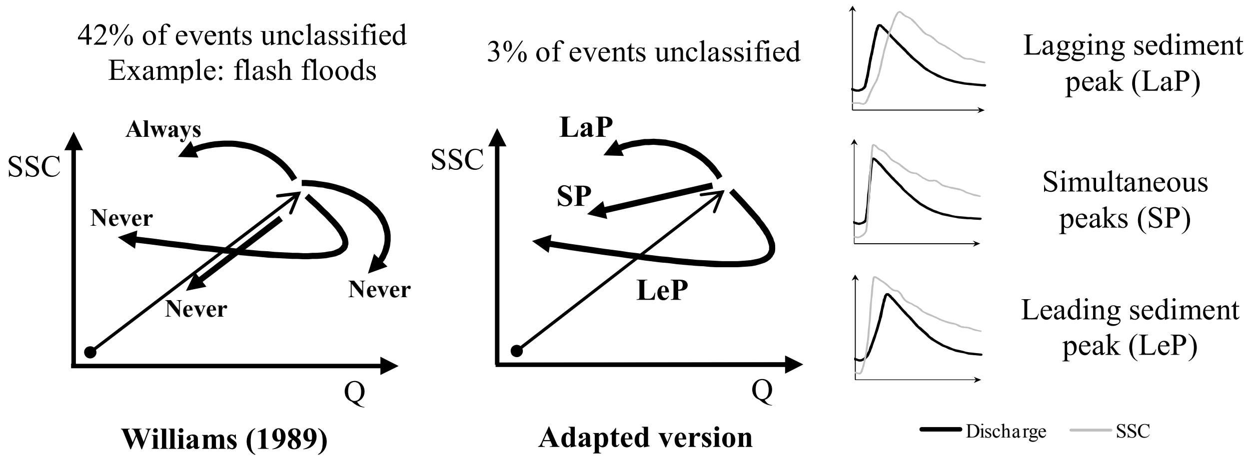
42% of events unclassified
Example: flash floods
Always
SSC
Never
Never
Never
Q
Williams (1989)
3% of events unclassified
LaP
SSC
SP
LeP
Q
Adapted version
Lagging sediment peak (LaP)
Simultaneous peaks (SP)
Leading sediment peak (LeP)
Discharge
SSC

991 Fig. 5

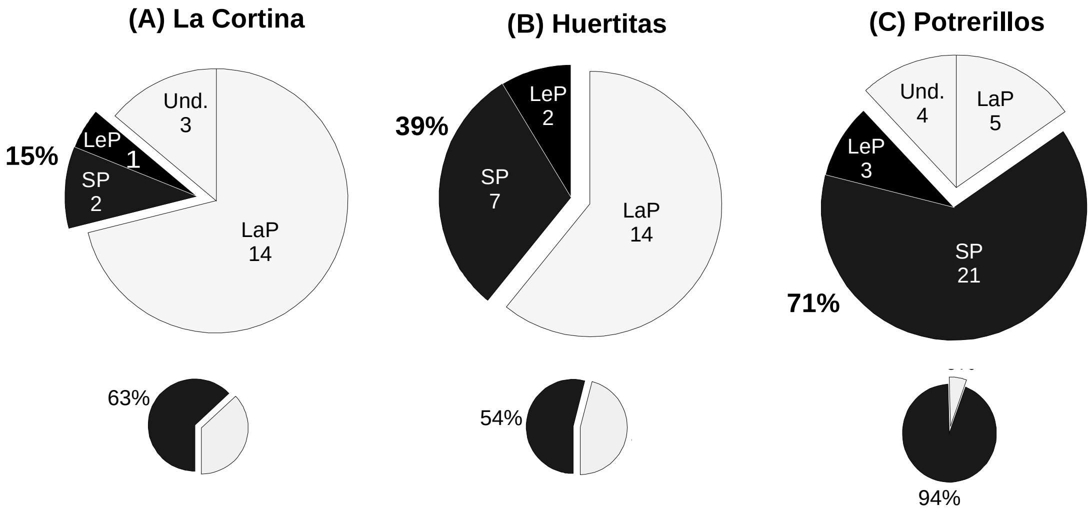
(A) La Cortina
Und.
3
LeP
1
SP
2
15%
LaP
14
63%
(B) Huertitas
LeP
2
39%
SP
7
LaP
14
54%
(C) Potrerillos
Und.
4
LaP
5
LeP
3
SP
21
71%
94%

992

Fig. 6

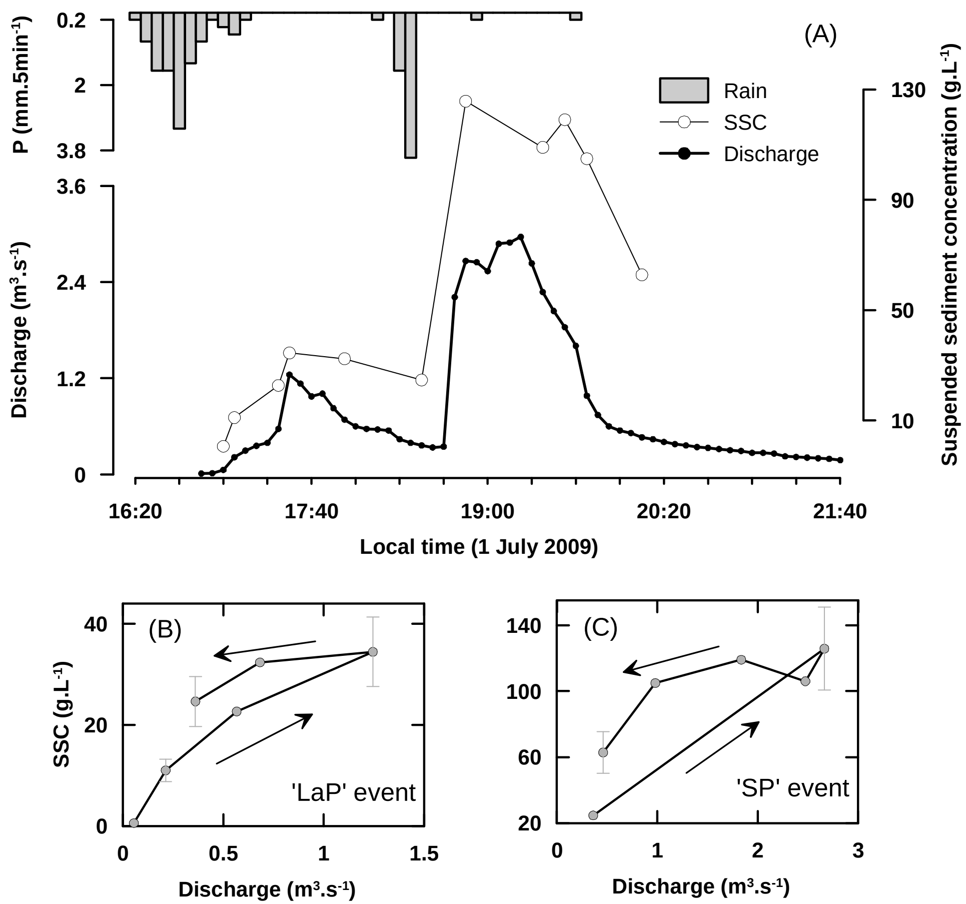
(A)
P (mm.5min-1)
0.2
2
3.8
Rain
SSC
Discharge
Discharge (m3.s-1)
3.6
2.4
1.2
0
Suspended sediment concentration (g.L-1)
130
90
50
10
16:20
17:40
19:00
20:20
21:40
Local time (1 July 2009)
(B)
SSC (g.L-1)
40
20
0
0.5
1
1.5
'LaP' event
Discharge (m3.s-1)
(C)
140
100
60
20
0
1
2
3
'SP' event
Discharge (m3.s-1)

Fig. 7

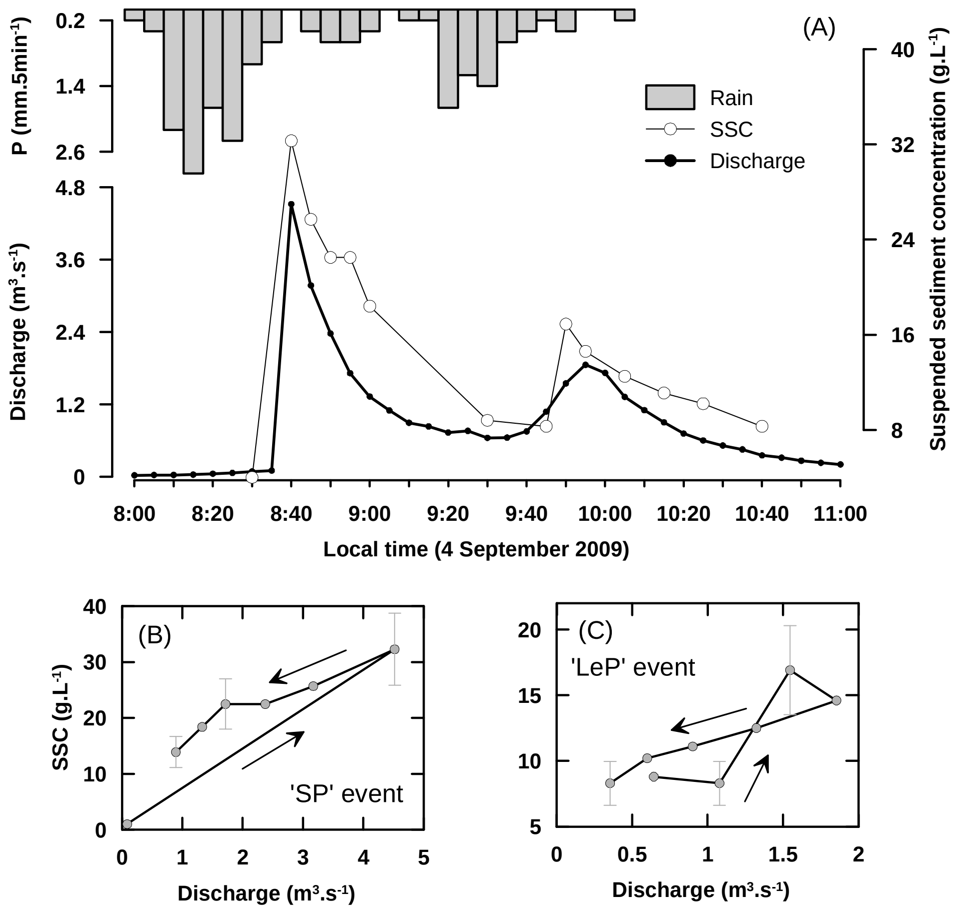
(A)
P (mm.5min-1)
0.2
1.4
2.6
Rain
SSC
Discharge
Discharge (m3.s-1)
4.8
3.6
2.4
1.2
0
Suspended sediment concentration (g.L-1)
40
32
24
16
8
8:00
8:20
8:40
9:00
9:20
9:40
10:00
10:20
10:40
11:00
Local time (4 September 2009)
(B)
'SP' event
SSC (g.L-1)
40
30
20
10
0
0
1
2
3
4
5
Discharge (m3.s-1)
(C)
'LeP' event
20
15
10
5
0
0.5
1
1.5
2
Discharge (m3.s-1)

Fig. 8

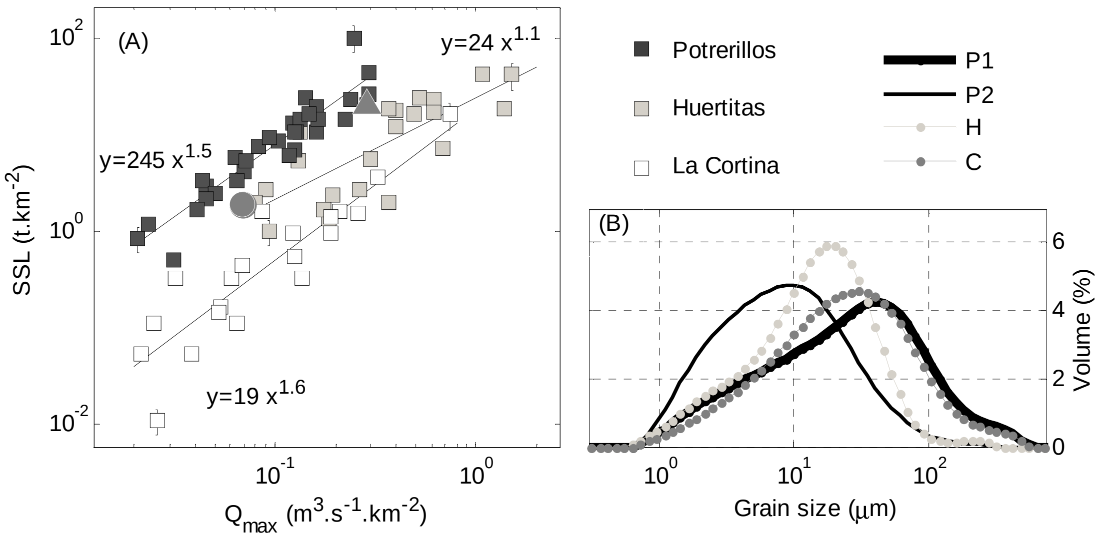

(A)
y=24 x1.1
y=245 x1.5
y=19 x1.6
SSL (t.km-2)
Qmax (m3.s-1.km-2)
Potrerillos
Huertitas
La Cortina
P1
P2
H
C
(B)
Volume (%)
Grain size (μm)

Fig. 9

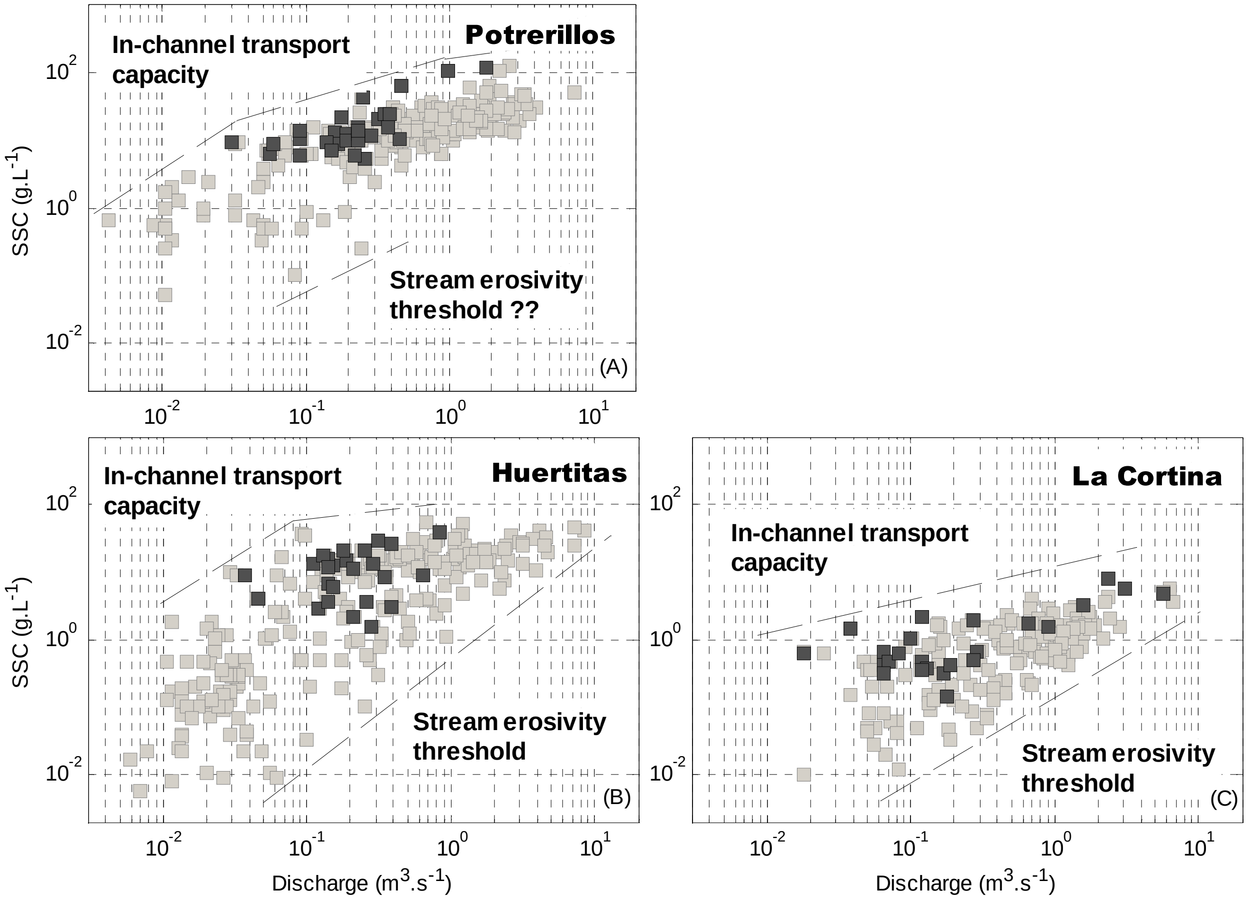
Potrerillos
In-channel transport capacity
Stream erosivity threshold ??
(A)
SSC (g.L-1)
Huertitas
In-channel transport capacity
Stream erosivity threshold
(B)
La Cortina
In-channel transport capacity
Stream erosivity threshold
(C)
Discharge (m3.s-1)
Discharge (m3.s-1)

1001 Fig. 10

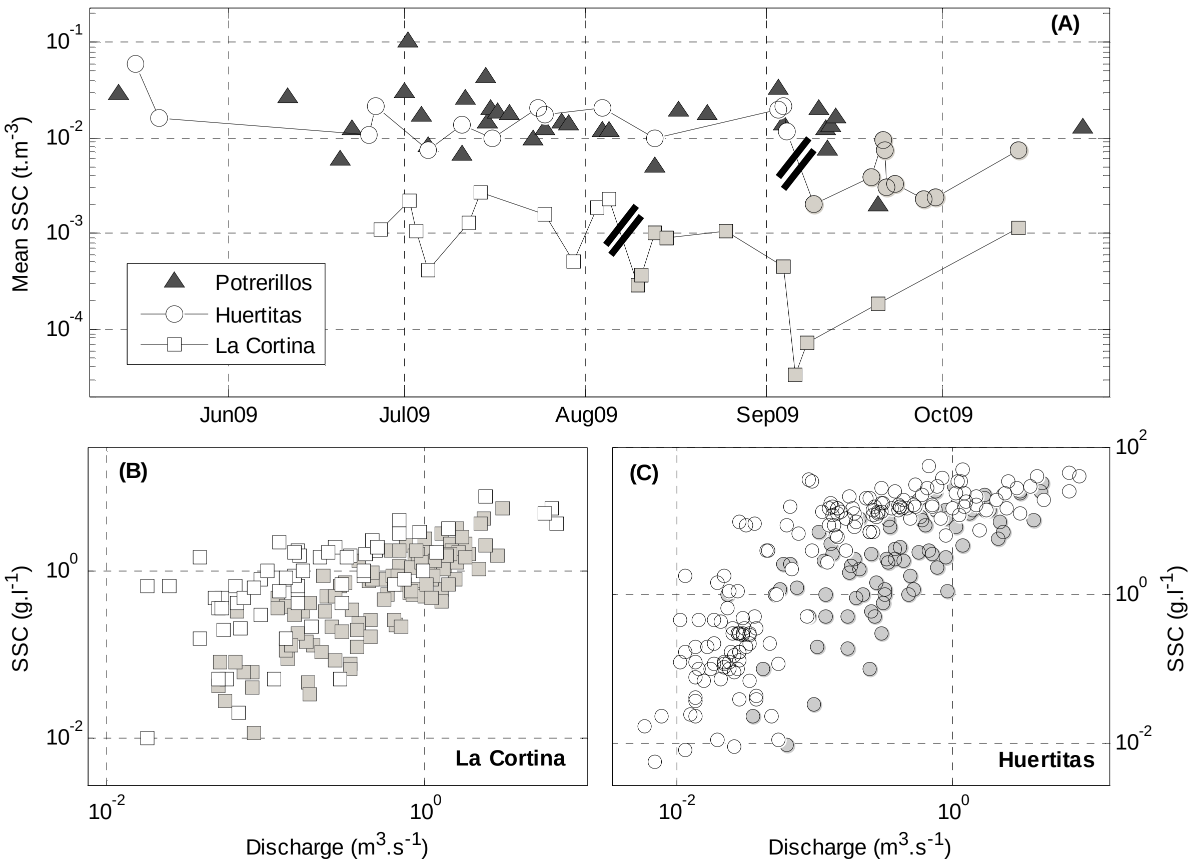

1002

Table 1

Main characteristics of the three study sites[a]

	Area (km^2)	Altitude range (m)	Mean slope (%)	Main land uses	Main soil types	Severely eroded areas (% of catchment surface)	Mean discharge during the dry season ($L.s^{-1}$)	Mean discharge during the wet season ($L.s^{-1}$)	Mean SSC ($mg.L^{-1}$)
La Cortina	9.3	2250-2700	12	Forest (52%), cropland (46%)	Andisols (100%)	0	10-30	100-200	5
Huertitas	3.0	2150-2450	18	Rangeland (65%), cropland (28%), gullied (6%)	Acrisols (100%)	6	0.05-1	10-30	30
Potrerillos	12.0	2200-2700	15	Cropland (40%), forest (37%), grassland (23%)	Acrisols (60%), Andisols (40%)	1	0	20-50	1000

[a] Data from the three last columns were collected during monthly surveys carried out in 2007 and 2008. The high mean SSC value in Potrerillos is a direct consequence of the ephemeral behaviour of the stream. Measurements could only be conducted immediately after storms and before the streams dried out.

Table 2

Semiquantitative parameters computed for each storm

Parameter	Description	Class
Flood characteristic	Hydrograph rising phase > 5 min	Slow
	Hydrograph rising phase < 5 min	Fast
Initial moisture conditions	Events without significant rainfall in the last 24 h	1 (dry)
	Significant rainfall (> 4 mm) without flood generation	2 (wet+)
	Significant rainfall (> 4 mm) with minor flood generation	3 (wet++)
	Significant rainfall (> 4 mm) with major flood generation	4 (wet+++)

Table 3

Estimation of the suspended sediment yields exported from the three study sites in 2009

Station	2009 sediment delivery (t)[a]	Area (km^2)	Specific suspended sediment yield (t.km^{-2}.y^{-1})[a]
La Cortina	300	9.3	30
Huertitas	2600[(1)] 4600[(2)]	3.0	900[(1)] 1500[(2)]
Potrerillos	7400[(1)] 9500[(2)]	12.0	600[(1)] 800[(2)]

[a] (1) refers to low estimates and (2) refers to high estimates (including the expected contribution of ungauged events).

Table 4

Suspended sediment yields measured in other small catchments

Subcatchment	Years of monitoring	Area (km^2)	SSY ($t.km^{-2}.y^{-1}$)	Reference
Lower Smisby	1997-1999	2.6	80	Walling et al., 2002
Rosemaund	1997-1999	1.5	82	Walling et al., 2002
Stanley Cars	1999-2001	4.6	94	Goodwin et al., 2003
Moulin	1988-2000	0.9	5700	Mathys et al., 2003
Brusquet	1988-2000	1.1	80	Mathys et al., 2003
Moulinet	2002-2003	4.5	25	Lefrançois et al., 2007
Violettes	2002-2003	2.2	36	Lefrançois et al., 2007
May Zegzeg	1998-2001	2.0	560	Nyssen et al., 2008
Flyers Creek	2005-2006	1.6	8	Smith, 2008